METEOROLOGICAL APPLICATIONS
Meteorol. Appl. (2012)
Published online in Wiley Online Library
(wileyonlinelibrary.com) DOI: 10.1002/met.1307

Simulation of a baroclinic wave with the WRF regional model: sensitivity to the initial conditions in an ideal and a real experiment

Josefina Blázquez,[a]* Natalia L. Pessacg[b] and Paula L. M. Gonzalez[c]

[a] *Centro de Investigaciones del Mar y la Atmósfera (CIMA/CONICET-UBA), Departamento de Ciencias de la Atmósfera y los Océanos (DCAO/FCEN), UMI IFAECI/CNRS, Ciudad Universitaria Pabellón II Piso 2, Buenos Aires, Argentina*

[b] *Centro Nacional Patagónico (CENPAT/CONICET), Puerto Madryn, Chubut, Argentina*

[c] *International Research Institute for Climate and Society, Earth Institute, Columbia University, Palisades, NY, USA*

ABSTRACT: A sensitivity study to perturbations in the initial conditions in a simulated evolution of a baroclinic wave using the Weather Research and Forecasting (WRF) regional model is discussed in this paper. With the goal of analysing the impacts of these perturbations in the context of weather forecast and also with the aim of exploring the presence of preferred directions of growth in the errors, two cases were analysed: an ideal experiment using a case study available from the WRF set-up and a simulation of a real evolution of a mid-latitude cyclone over Southeastern South America (SESA) and the Atlantic Ocean. In the ideal experiment two spatial structures were considered for the perturbations, random and sinusoidal noise, while for the real experiment only sinusoidal structures were considered. These perturbations were then applied to the initial conditions of temperature and zonal wind. Additionally, simulations with an increment in atmospheric moisture were performed for the real experiment. It was found in both real and ideal cases that the temperature errors tend to organize in a preferable direction of growth, although this direction changes depending on the case considered. Results also show that perturbations in temperature field lead to larger error than perturbing the zonal wind. Finally, the increment of moisture did not produce significant changes in the distribution or intensity of the errors in the real case. Copyright © 2012 Royal Meteorological Society

KEY WORDS perturbations; WRF model; error growth; Southeastern South America; cyclone; initial conditions

Received 14 June 2011; Revised 29 December 2011; Accepted 31 January 2012

1. Introduction

Lorenz (1963a, 1963b) discovered that the atmosphere, like any unstable dynamic system, has a finite limit in its predictability. This limit is associated with the intrinsic chaotic behaviour of these dynamic systems and it is present even considering a full physics model and quasi-perfect initial conditions (as reanalysis or observations).

In the atmosphere, predictability depends on the scale of the system. In the case of the mesoscale, the fast error growth and the strong sensitivity, even to random perturbations to the initial conditions, make it difficult to control the convergence of the forecast. The synoptic scale, however, presents a different behaviour. The error growth in this scale is slower than in the mesoscale, it is less sensitive to random perturbations and it has few preferential directions of growth compared with the number of system variables. Patil *et al*. (2001) found that in a very unstable situation, such as cyclogenesis, the number of directions of maximum growth decreases (between one or two).

The fact that small perturbations in the initial conditions have the potential to generate large differences in the numerical predictions motivates the generation of sensitivity studies to evaluate such potentiality for distinctive dynamical configurations.

* Correspondence to: J. Blázquez, Departamento de Ciencias de la Atmósfera y los Océanos (DCAO/FCEN), Centro de Investigaciones del Mar y la Atmósfera (CIMA/CONICET-UBA), UMI IFAECI/CNRS, Ciudad Universitaria Pabellón II Piso 2, C1428EGA Buenos Aires, Argentina. E-mail: blazquez@cima.fcen.uba.ar

It has been demonstrated that changes in the initial conditions determine different results in model predictions (Zhang *et al*., 2002; Tan *et al*., 2004) and as a result their accuracy is of major importance, especially in weather forecasts (Zhu and Thorpe, 2006). These authors have described forecast error growth in the mesoscale, associated with model imperfection and initial conditions uncertainty, using an empirical model that separates the error due to the initial conditions and the portion due to the model deficiencies. They found that over the lifetime of the cyclone it is important to have accurate initial conditions to be able to forecast the cyclone development with some skill.

The present work introduces a sensitivity study to perturbations in the initial conditions in an idealized experiment considering a 3D baroclinic wave on a baroclinically unstable jet, and compares these results with a simulation of an observed cyclogenesis affecting Southeastern South America (SESA). In contrast with previous work (Zhang *et al*., 2002; Tan *et al*., 2004; Zhu and Thorpe, 2006) the results of the present paper were focused on the synoptic scale and were concentrated in assessing the impact of perturbing initial conditions in the quality of weather forecasts. The occurrence of cyclogenesis is of great relevance in SESA, since these events significantly contribute to modulation of weather and climate (Mendes *et al*., 2010). According to Gan and Rao (1991), Sinclair (1995) and Mendes *et al*. (2010) one of the main areas in South America for enhanced cyclogenesis is in between 25° and 40 °S, near the coast of Argentina, Uruguay and south of Brazil. It has been demonstrated that the reason for the preferential development of the cyclones in that area is the baroclinic

instability of the westerlies and the orographic effects provided by the Andes chain (Bonatti and Rao, 1987; Gan and Rao, 1991, 1994; Sinclair, 1995). Previous studies have also shown that the seasons with the highest activity of these systems are winter and summer (Mendes *et al*., 2010). The extratropical cyclones significantly contribute to seasonal precipitation totals and are often related to weather extremes over SESA. Vera *et al*. (2002) found that more than 60% of the mean winter accumulated precipitation could be attributed to the cyclonic disturbances and Possia *et al*. (2003) analysed a superstorm which occurred on May 2000 over La Plata River, which produced a record in 24 h accumulated precipitation in Concordia city (31.18 °S, 58.01 °W) and hurricane-force winds in the studied area. Occasionally, these systems are also related to a particular phenomenon called 'Sudestada', which consists of strong south-easterly winds over the La Plata River that push the water of the river to the lowlands, causing flooding in Buenos Aires city and its surroundings. Ciappesoni and Salio (1997) have documented this phenomenon and they found that the Sudestada is always accompanied by a high pressure over the Patagonia region and often with a low pressure system over the northeast of Argentina.

Within this framework, the present paper aims to assess the impact of perturbing the initial conditions when simulating this kind of systems in the context of weather forecast and to explore the presence of preferred directions of growth in the errors.

In addition, the following questions are introduced throughout the study:

- are the differences between perturbing temperature and zonal wind initial conditions comparable between the real and the idealized simulations;
- is there a preferred direction of error growth in the real case? If so, is it analogous to the one observed in the idealized experiment, and,
- do moist processes play a relevant role in error growth?

This paper is organized as follows. Section 2 presents the model description and the experimental design. The results based in the ideal and the real cases are discussed in Section 3. Finally, the discussion and conclusions of this study are given in Section 4.

2. Model description and experimental design

For both real and ideal experiments, the WRF (Weather Research and Forecasting) regional model was used. WRF version 3.0.1 (Skamarock *et al*., 2008) was employed to simulate the real case, whereas the ideal experiment was run with version 2.2 (Skamarock *et al*., 2005). This last version simulates the evolution of a 3D baroclinic wave within a baroclinically unstable jet in the northern hemisphere, under an f-plane approximation. The experiment was performed for the northern hemisphere because in the ideal pack that the WRF model provides, the user can only change the parameterizations whereas the rest of the experimental design (the boundary and initial conditions, the domain size and location, the resolution and the vertical levels) are fixed. The model was run using a mesh of 41 points in the zonal direction and 81 in the meridional one, with a horizontal resolution of 100 km. The vertical grid has 25 levels and a fixed top at 16 km. The boundary conditions are symmetric in the north–south direction. This treatment of the boundary conditions corresponds to the physical assumption that the same physical processes exist on the two sides of a boundary. In the west-east direction the boundary conditions are periodic. In all the simulations, parameterizations for cloud microphysics only (Kessler scheme based on Kessler, 1969) and cumulus convection (Kain–Fritsch scheme based on Kain-Fritsch, 1990, 1993) were considered. Each simulation had a length of 6 days.

In the case of the real experiment, the regional model was run using the NCEP GDAS (Global Data Assimilation System) analysis as boundary and initial conditions, with a horizontal resolution of $1^\circ \times 1^\circ$. The simulation started on 5 November 2006 at 1200 UTC and finished on 9 November 2006 at 0000 UTC. The period of integration was chosen in order to explore the impact of perturbing initial conditions in weather prediction, independently of the stage of development of the cyclonic perturbation or of whether the system qualifies as the most unstable mode according to the baroclinic instability theory. Simulations were done applying a one-way nesting technique. The experimental domain is located over southern South America (Figure 1). The domain has a size large enough to study the growth of the perturbations, i.e. the results in the inner domain are not affected by the boundary conditions. The parent domain has a grid spacing of 60 km and the inner domain has a horizontal resolution of 20 km. The analysis of the simulations was done without considering a spin up period as it would have been done in the context of weather forecasting. The Kessler scheme was used to parameterize cloud microphysics, the Kain–Fritsch scheme for cumulus convection and Mellor-Yamada-Janjic scheme (Mellor and Yamada, 1982; Janjic, 1990, 1996, 2002) for the planetary boundary layer parameterization. The land-surface is described by the Noah model (Chen and Dudhia, 2001).

To analyse the influences of the initial conditions in the simulation of cyclogenesis in the real and the ideal cases, several experiments were carried out as shown in Table 1, for the ideal case, and Table 2, for the real simulation. In the ideal experiment, two spatial structures were considered for the perturbations: random and sinusoidal noise. These perturbations were then applied to the initial conditions of different atmospheric variables. As an example, Figure 2 displays a set of perturbations introduced to the temperature initial conditions in the ideal case. Maxima of 2 °C can be seen in Figure 2 for the sinusoidal and random experiments. The same procedure was

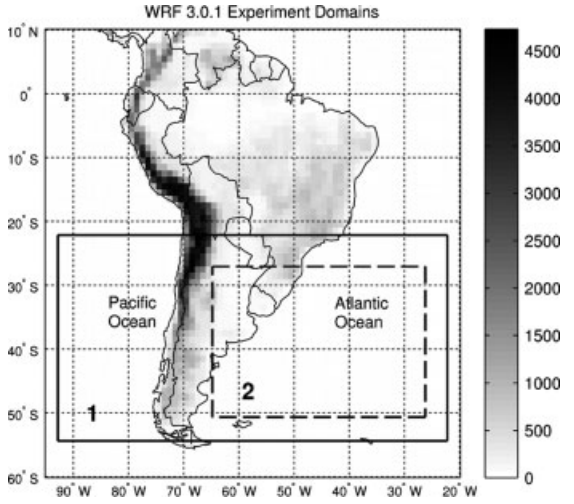

Figure 1. Model domains for the real experiments. Number 1 stands for parent domain and 2 for inner domain. Grey shading represents observed topography in metres.

Table 1. Ideal case experiments.

Experiments for ideal case (i)	Description of the experiments	Temperature all levels random	Temperature all levels sinusoidal	Zonal wind all levels random	Zonal wind all levels sinusoidal
CTLi	Control experiment	No	No	No	No
PTRi	Temperature perturbed randomly	Yes	No	No	No
PTSi	Temperature perturbed sinusoidally	No	Yes	No	No
PURi	Zonal wind perturbed randomly	No	No	Yes	No
PUSi	Zonal wind perturbed sinusoidally	No	No	No	Yes

Table 2. Real case experiments.

Experiments of real case	Description of the experiments	Temperature all levels	Temperature 1 level	Temperature exponential with levels	Zonal wind all levels	Change of moisture (10% increase in the entire mixing ratio profile)
CTL	Control experiment	No	No	No	No	No
CTLH	Control experiment with increased humidity	No	No	No	No	Yes
PTS	Temperature perturbed sinusoidally	Yes	No	No	No	No
PTS1lev	Temperature perturbed sinusoidally in one level (surface)	No	Yes	No	No	No
PTSexp	Temperature perturbed sinusoidally with vertical exponential decrease in its amplitude	No	No	Yes	No	No
PUS	Zonal wind perturbed sinusoidally	No	No	No	Yes	No
PTSH	Temperature perturbed sinusoidally and increased of humidity	Yes	No	No	No	Yes
PUSH	Zonal wind perturbed sinusoidally and increased of humidity	No	No	No	Yes	Yes

repeated for the zonal wind, where the maximum perturbation reached a value of 2 m s^{-1} in the random case and 0.8 m s^{-1} in the sinusoidal experiment (not shown). The choice of sinusoidal and random perturbations in the ideal case was done with the aim of comparing the impact of spatially organized *versus* unorganized errors. The adoption of temperature and zonal wind as the variables to be perturbed in both experiments was done in order to compare how an error in the movement field *versus* an error in the mass field can affect the solution. In the real experiment only sinusoidal perturbations were applied to the zonal wind and temperature initial conditions, based on the results obtained for the previous experiment. In addition, in the real case, a simulation increasing the mixing ratio profile of all the levels by 10% was done to check how the sinusoidal perturbations would impact on a more unstable atmosphere. After perturbing the moisture field, super-saturation conditions were not found in any grid point. To analyse the impact of introducing perturbations with amplitudes depending on the vertical levels, two extra experiments were done in the real case: one perturbing only the first level of the temperature field and the other perturbing the temperature field exponentially with height. It is worth clarifying that the set of initial perturbations used in this work would not be proper for an ensemble design, since the perturbations are not balanced and the geostrophic adjustment would remove most of the associated energy quickly. The intention here is to account theoretically for the impact of unknown and uncontrolled errors.

The maximum amplitudes in both the sinusoidal and random perturbations were chosen to be a fraction of the day-to-day standard deviation obtained using the NCEP/NCAR Reanalysis in the period 1979–2010 for the region of genesis of the systems. These values ensure that the perturbations introduced to the temperature and zonal wind initial conditions are comparable.

3. Results

3.1. Ideal case

As mentioned previously, this experiment was run using one of the ideal packages that are available in the WRF model.

This ideal case is characterized at the initial time for a typical jet structure at upper levels, with a maximum of 65 m seg^{-1}, and a baroclinic zone which will lead to the amplification of the wave. In the incipient stage of the cyclone, the mid- and low-level flows are characterized by a wave trough. When the system finally closes at surface level (day 3) the upper level still shows a wave trough but tilted to the west. The cyclone reaches its mature stage after almost 6 days of integration (132 h), showing a barotropic structure. At this time, the magnitude of the temperature (sea level pressure) anomalies in the control simulation are between −20 and 10 °C (−70 and 20 hPa).

Figure 3 shows differences between randomly perturbed and control simulations (PTRi-CTLi and PURi-CTLi) at 132 h of simulation for temperature, pressure and precipitation. When temperature initial conditions are modified (Figure 3(a), (c) and (e)), the differences between perturbed and control simulations are bigger than when the zonal wind field is perturbed (Figure 3(b), (d) and (f)). As shown in Figure 3(a), the largest errors are in the east–west direction. This structure is mainly due to the fact that the cyclone is positioned further west with respect to the control simulation when the temperature field was perturbed randomly. This distribution of errors is not observed in the PURi experiment (Figure 3(b)). On the contrary, a weak

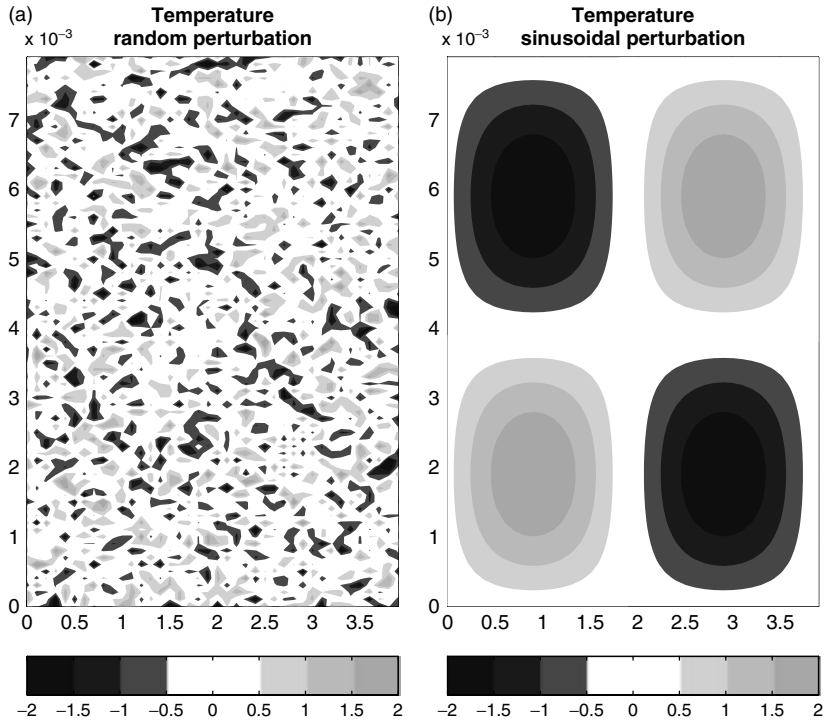

Figure 2. Perturbations introduced to the temperature initial conditions in the ideal experiment for cases: random (a), sinusoidal (b). Units are °C. The scaling factor (10^{-3}) corresponds to the spatial dimensions.

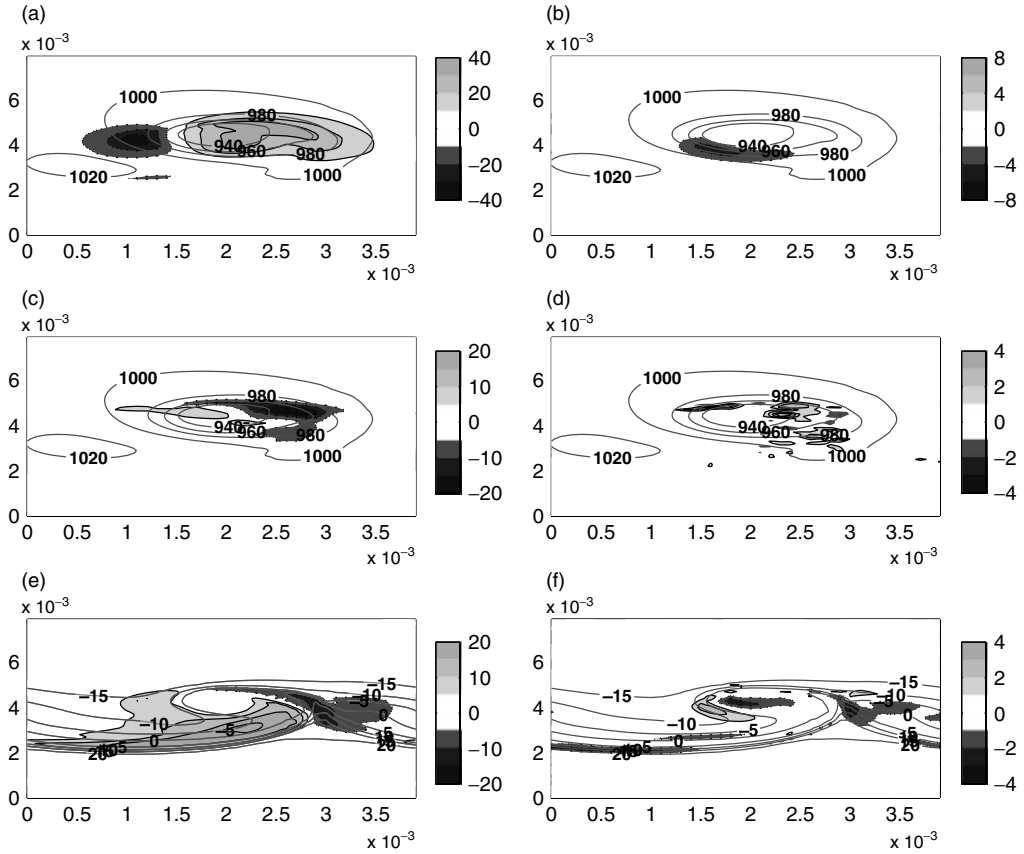

Figure 3. Differences between perturbed and Control experiments (PTRi-CTLi: left panels and PURi-CTLi: right panels) (shaded) at 132 h of simulation. (a) and (b) pressure at 500 m (hPa), (c) and (d) precipitation (mm) (e) and (f) temperature at 500 m (°C). Contour lines in (a), (b), (c) and (d) indicate the pressure (hPa) in CTLi experiment and contour lines in (e) and (f) indicate temperature (°C) for CTLi simulation. The scaling factor (10^{-3}) corresponds to the spatial dimensions.

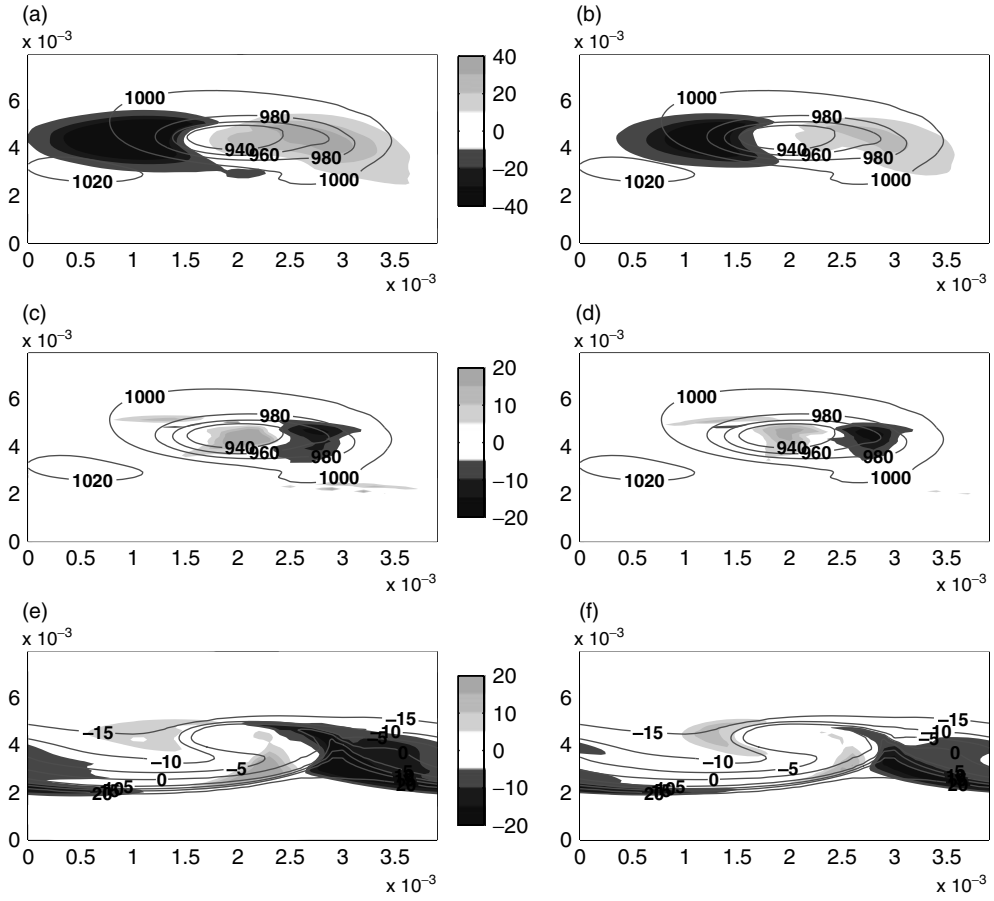

Figure 4. Same as Figure 3 but for differences between perturbed and Control experiments (PTSi-CTLi: left panels and PUSi-CTLi: right panels).

difference between the CTLi and PURi simulations is found to the southwest, indicating that when the zonal wind was perturbed randomly the cyclone trajectory did not suffer substantial changes. The rest of the figures display the precipitation (Figure 3(c) and (d)) and temperature differences (Figure 3(e) and (f)) showing an agreement with the displacement of the cyclone. As mentioned previously, the perturbations to the temperature and zonal wind initial conditions are comparable, so that the differences in the response in the different experiments are solely due to the dynamical response of the model. This particular configuration of the system appears to be more sensitive to perturbations in a mass variable than to errors in the momentum variables, and this may be related to the particular choices of parameterizations or to the non-linearities of the system. Nevertheless, the results analysed here are only valid to this particular case study and this set of idealized perturbations, and only allow hypothesis of similarities with the behaviour of analogous systems.

When a sinusoidal noise structure was added to the initial conditions (Figure 4), the errors tended to be larger than in the random case. This increase in the error magnitude is mainly due to the cyclone's movement further to the west than in the random experiment.

It is worth mentioning that the errors found in Figures 3 and 4 have the same order of magnitude than the anomalies of the baroclinic wave.

These preliminary results lead to the conclusion that in this idealized case the spatial distribution of the errors is independent of the spatial structure of the perturbations in the case of temperature, showing a preferred direction of growth. In the case of perturbations introduced to the zonal wind, no significant changes were observed when a random structure was chosen.

To explore the temporal evolution of the errors, quadratic differences of temperature, pressure, zonal wind and precipitation were computed. Figure 5 displays the time series of the quadratic differences averaged over the target domain between the perturbed and control experiments. It can be seen that the error magnitude for all of the variables is bigger in the experiments with sinusoidal perturbations than in simulations with random structures. In addition, if temperature and zonal wind perturbed simulations are compared the error is larger when the temperature initial field is perturbed. It also can be seen from Figure 5 that random perturbations to the zonal wind do not produce significant departures from the control simulation. As noted previously, this behaviour could be due to the fact that under this ideal conditions perturbing the zonal wind lead to less error than perturbing temperature.

3.2. Real case

The study was completed by simulating a real cyclogenesis to evaluate the impact of the perturbations in the initial conditions and to compare such impact with the ones observed in the idealized experiment. The period chosen corresponds to a cyclogenesis that developed over SESA and moved towards the southeast to the Atlantic Ocean. The low-pressure system reaches its mature stage on 8 November at 0600 UTC, which matches with 66 h of simulation. At this time, the system presents a barotropic structure. The upper- and mid-level flows

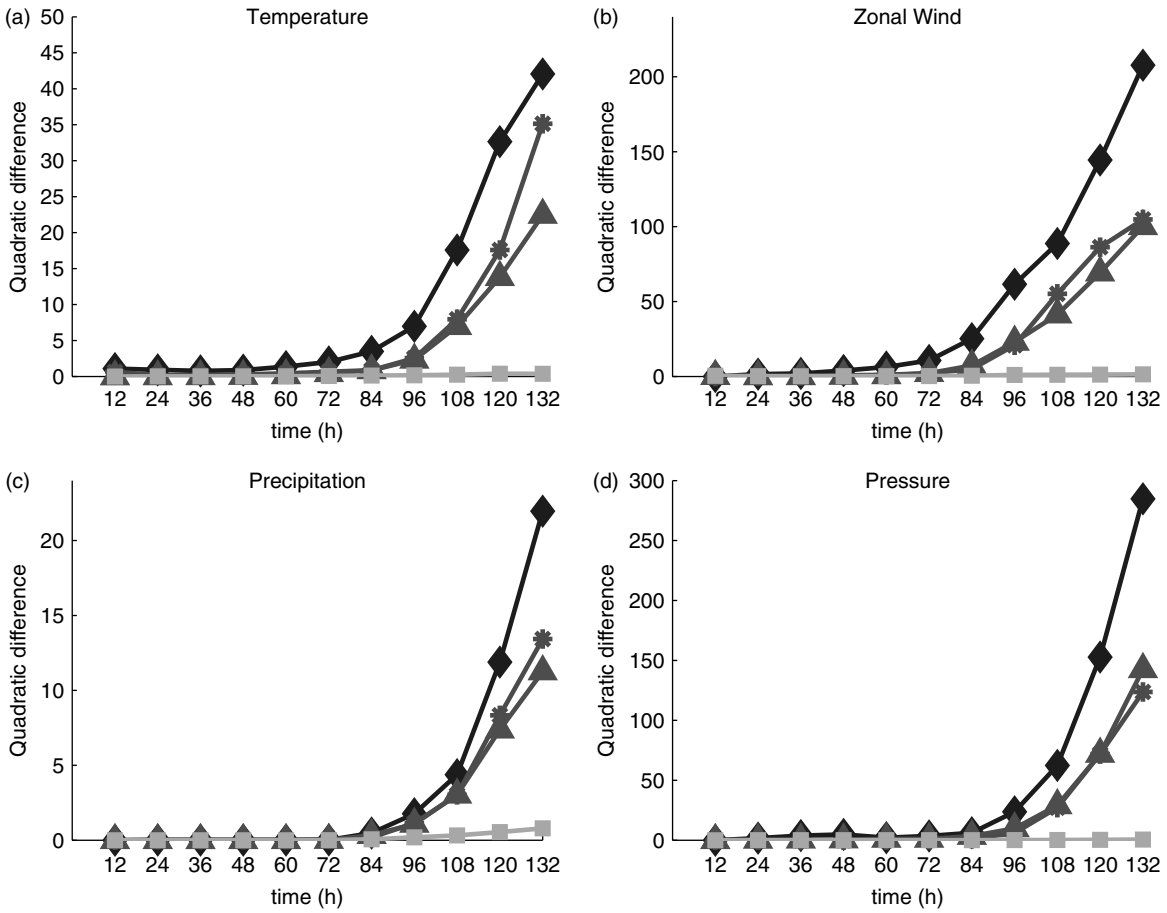

Figure 5. Series of quadratic differences between perturbed and control simulations. (a) Temperature (2 °C), b) pressure (2 hPa), c) zonal wind ($m^2\ s^{-2}$), at 500 m and (d) precipitation (mm^2). Diamond indicate PTSi, circle PTRi, triangle PUSi and square PURi.

before the mature stage are characterized by a wave trough that moved slowly to the east. In addition, these upper and mid-level waves are tilted to the west with respect to the surface's cyclone. The evolution of this system does not match with the characteristics of the explosive mid-latitude cyclogenesis.

Of all the configurations considered in the ideal experiment, the case in which a sinusoidal perturbation structure was added to the temperature initial field is the one that resulted in the larger error amplitudes. For this reason, only sinusoidal perturbations were added to the initial condition fields in the real case. For more details of the real experiments see Table 2. Figure 6 shows the evolution of the geopotential height differences between the PTS and CTL runs (Figure 6(a)) and between the PUS and CTL runs (Figure 6(b)). It can be seen from the figure that the cyclone was shifted to the southeast (northwest) in the case where the perturbation was applied to temperature (zonal wind). The errors in precipitation (not shown) do not present a coherent spatial structure and as a consequence cannot be directly attributed to the changes in geopotential height. Figure 7 shows the evolution of the geopotential height differences between the PTSH and CTLH runs and between PUSH and CTLH. It can be seen from this figure that the increase in moisture in the initial condition did not yield a significant impact on the evolution of this variable, given that the distribution of the error is similar to the one observed in the experiments with unperturbed humidity. This result disagrees with those found by Zhang *et al*. (2002) and Tan *et al*. (2004), who have concluded that the inclusion of moisture in a similar experiment was characterized by an up-scale error growth. Such difference can be due to the fact the authors simulated an explosive cyclogenesis, for which moist processes gain relevance. Therefore, it could be hypothesized that the main dynamic mechanism associated with the cyclone evolution simulated in this work could be dry baroclinic instability.

To explore the influence of the perturbations on precipitation fields, the bias was calculated following Wilks (1995):

$$Bias = \frac{P}{C} \tag{1}$$

P (C) indicates the number of grid points with precipitation bigger than 0.01 mm in the perturbed experiments (control run). Therefore, values of 1 indicate that the quantity of grid points with precipitation is equal for both the control and the perturbed simulations. Figure 8 displays the bias of precipitation for all the experiments and the number of grid points with precipitation greater than 0.01 mm in CTL and CTLH experiments. The figure shows that the PTS and PTSH simulations exhibit precipitation biases larger than 1 after 36 h of simulation, whereas the PUS and PUSH experiments show values lower than 1 during most of the simulation period (with the exception of PUS at 18 and 48 h and PUSH at 54 h). These lead to the conclusion that in the last hours of simulation, when temperature (zonal wind) field is perturbed, precipitation coverage increases (decreases) with respect to control simulations. In general, the PTS1lev and PTSexp simulations show values of bias around 1, pointing out that perturbed and control simulation have almost the same quantity

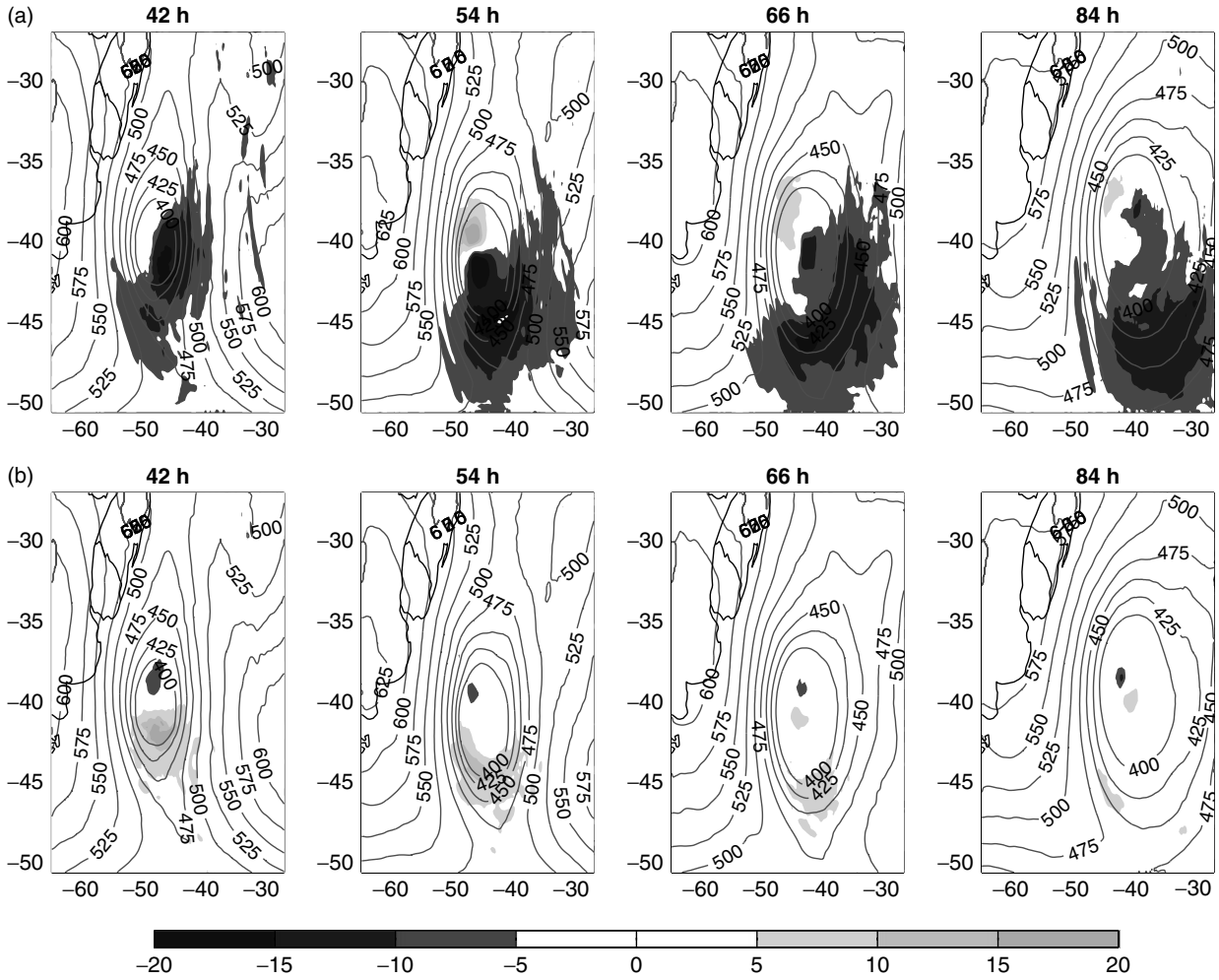

Figure 6. (a) Differences of 950 hPa geopotential height between PTS and CTL experiments (shaded), (b) differences of 950 hPa geopotential height between PUS and CTL experiments (shaded). Contour in (a) and (b) represents geopotential height in the CTL experiment. Units are geopotential metres.

of grid points with precipitation. The figure also shows that PTSH and PTS have larger biases (larger or smaller than 1) than the other experiments. There is no sign in the precipitation field that the increment of moisture leads to important changes in the distribution of the errors. Finally, it is worth mentioning that the number of points with precipitation ensured the robustness of the bias.

The cyclone trajectories were also calculated by identifying the grid point with the minimum sea level pressure in the inner domain of Figure 1. Figure 9 only shows the ones corresponding to experiments CTL, PTS, PUS, PTS1lev and PTSexp. The trajectories of the simulations with additional moisture have not been considered because no significant differences in the cyclone path were observed when humidity was perturbed. It can be seen from this figure that PTS1lev and PTSexp are the experiments with less variation in trajectory with respect to CTL simulation. On the other hand, PTS shows the greatest differences in its trajectory after 42 h of simulation. The results of this figure are in agreement with Figure 6, which shows a displacement of the cyclone to the southeast (northwest) in PTS (PUS) experiment. It also can be seen from Figure 9 that the cyclone's trajectories of perturbed experiments do not suffer substantial changes if they are compared with the control simulation. So, it could be said that the main differences that were found in Figures 6 and 7 are due to the intensification or deepening of the cyclone in perturbed simulations. This result disagrees with the findings for the ideal case.

4. Discussion and conclusions

A sensitivity study to initial conditions in the evolution of a cyclogenesis is presented in this paper. Several simulations were performed using the WRF regional model to explore the error growth in both ideal and real cases.

In the case of the ideal experiment, the cyclone shows a displacement to the west when the initial conditions are perturbed, both in the sinusoidal and random noise experiments. This behaviour was particularly noticeable when the temperature field was perturbed. The biggest errors were found when a sinusoidal perturbation was applied to the initial condition. By comparing temperature and zonal wind perturbations it was found that error growth was more important in the former. In conclusion, the biggest error growth was found when a sinusoidal perturbation was added to the temperature initial field. It was also found (especially for temperature) that irrespective of the perturbation applied to the initial condition, the errors always showed a west-east direction of maximum growth.

Taking into account the results from the ideal case, only sinusoidal perturbations were considered in the real experiments and

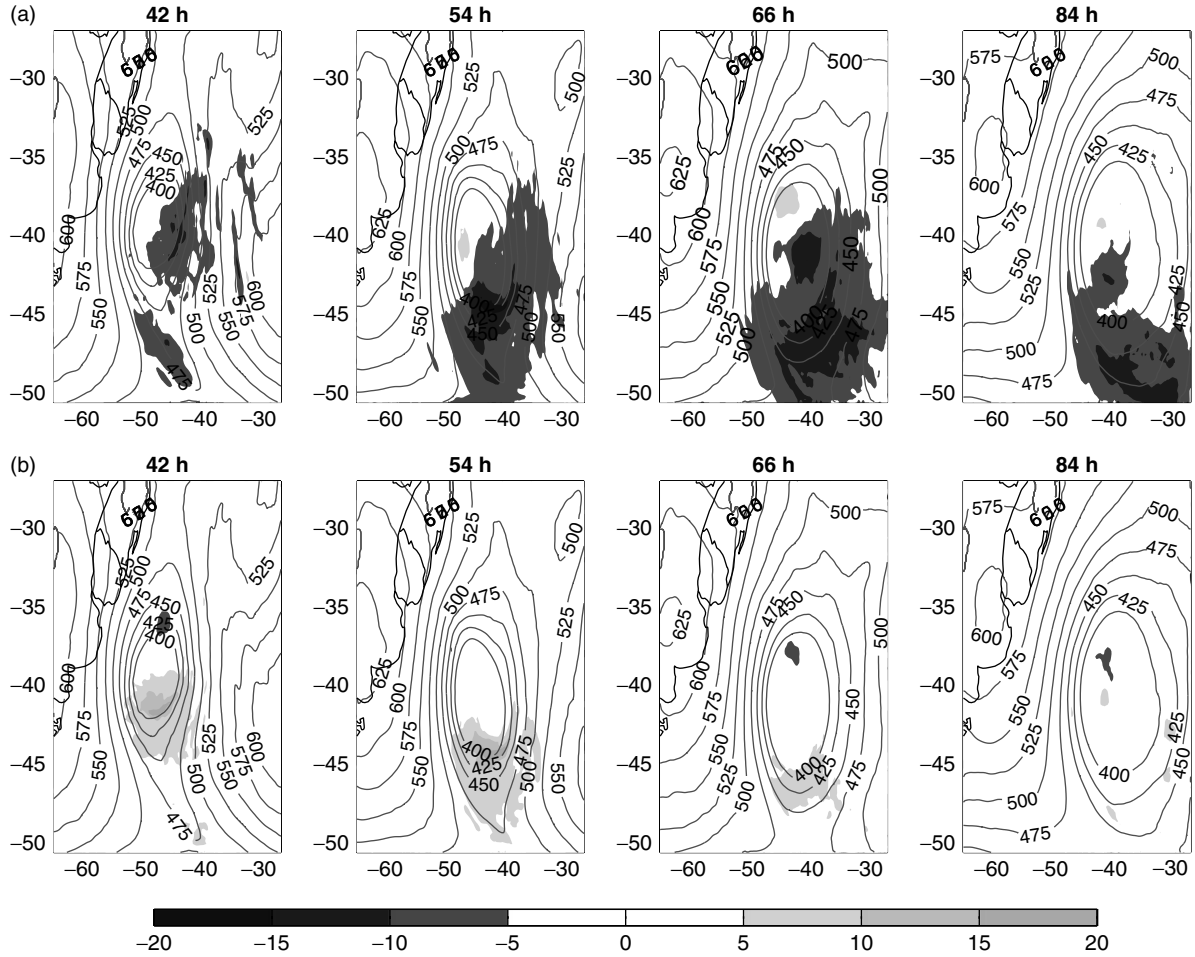

Figure 7. Same as Figure 6 but for the experiments with increased humidity. (a) PTSH-CTLH, (b) PUSH-CTLH.

more experiments applying a perturbation to the temperature initial field were performed (PTS1lev and PTSexp). In the real case, it was found that the cyclone was shifted to the southeast (northwest) when temperature (zonal wind) perturbation was added to the initial condition. As in the ideal case, errors tend to be organized in a preferable direction (northwest-southeast), independently of the perturbation added to the initial condition. The increase in the vertical profile of mixing ratio did not introduce significant changes in the distribution of the errors since the movement and intensity of the cyclone were not affected.

Precipitation bias was also analysed. It was found that PTS and PTSH experiments had more precipitation than the control experiments (CTL and CTLH, respectively), whereas PUS and PUSH simulations presented values of bias lower than 1, exhibiting less precipitation than CTL and CTLH experiments. These features are particularly noticeable in the last hours of simulation. As noted previously, the modification of the humidity did not lead to any relevant changes in the precipitation fields. Regarding cyclone trajectories, the greatest differences were found after 42 h in the PTS experiment. Nevertheless, even when some changes in the position of the cyclone centre were observed, the overall trajectory of this particular system was not very sensible to the perturbations to the initial conditions.

Going back to the questions presented in the introduction, the results suggest that although in ideal and real experiments the errors have organized in a preferable direction of growth, it can be seen that they are different (northwest-southeast in the real case and west-east in the ideal case), which could be due to particular features of the regional dynamics (topography, mean state, synoptic perturbations) that were present in both experiments when the model was initialized. To explore whether the intensity of errors in both ideal and real cases would be comparable, some variables were analysed and it was found that errors in a sinusoidally perturbed temperature field was much

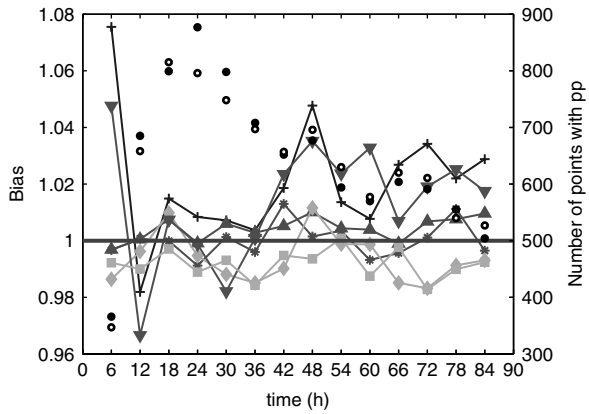

Figure 8. Precipitation bias for all the real experiments. PTS (plus sign); PTS1lev (asterisk); PTSexp (triangle); PUS (diamond); PTSH (reverse triangle); PUSH (square). Black closed circles and black open circles are number of grid points with precipitation larger than 0.01 mm in CTL and CTLH experiment respectively.

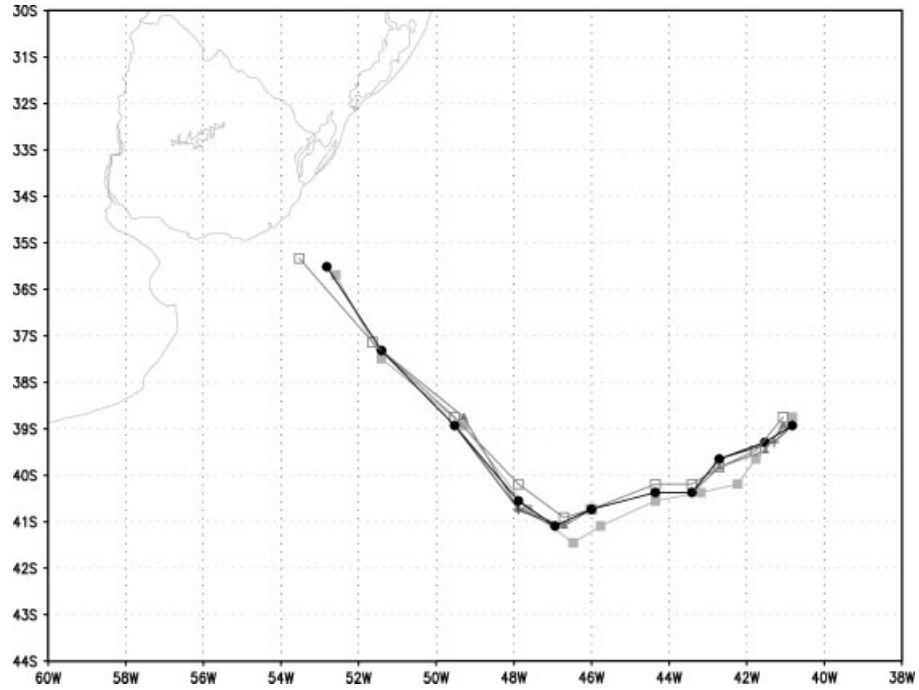

Figure 9. Cyclone trajectories for the experiments CTL (closed circle), PTS (closed square), PUS (opened square), PTS1lev (closed triangle) and PTSexp (plus sign), starting at 24 h of simulation (6 November 2006 at 1200 UTC) with marks every 6 h.

greater in the ideal than in the real case. This would mean that the errors intensity could be associated to the baroclinicity that each situation presents. These results allow the conclusion that differences between perturbing temperature and zonal wind initial conditions are not comparable between real and ideal cases. The inclusion of moisture in the real case does not lead to any significant changes, neither in the distribution nor in the intensity of the precipitation errors. This could be due to the fact that moist processes appear not to be dominating the evolution of the cyclone (during the period of analysis).

Finally, it is important to highlight that the previous results are case-dependent and different conclusions could be obtained if analysing a different system.

Acknowledgements

The authors would like to thank Juan Ruiz, Claudia Campetella and Ramiro Saurral for their comments and support. The research leading to these results has received funding from the European Community's Seventh Framework Programme (FP7/2007-2013) under Grant Agreement N° 212492: CLARIS LPB. A Europe-South America Network for Climate Change Assessment and Impact Studies in La Plata Basin. Finally, the authors are grateful to Dr. Silvina Solman and an anonymous reviewer whose comments and suggestions contributed to the improvement of this work.

References

Bonatti JP, Rao VB. 1987. Moist baroclinic instability in the development of the North Pacific and South American intermediate-scale disturbances. *J. Atmos. Sci.* **44**: 2657–2667.

Ciappesoni H, Salio P. 1997. Pronóstico de Sudestadas en el Río de la Plata. *Meteorologica* **22**(2): 67–81.

Chen F, Dudhia J. 2001. Coupling an advanced land-surface/hydrology model with the Penn State/NCAR MM5 modeling system. Part I: model description and implementation. *Mon. Weather Rev.* **129**: 569–585.

Gan MA, Rao VB. 1991. Surface cyclogenesis over South America. *Mon. Weather Rev.* **119**: 1293–1302.

Gan MA, Rao VB. 1994. The influence of the Andes Cordillera on transient disturbances. *Mon. Weather Rev.* **122**: 1141–1157.

Janjic ZI. 1990. The step-mountain co-ordinate: physical package. *Mon. Weather Rev.* **118**: 1429–1443.

Janjic ZI. 1996. The surface layer in the NCEP Eta Model. *Eleventh Conference on Numerical Weather Prediction, Norfolk, VA, 19–23 August 1996*. American Meteorological Society: Boston, MA; 354–355.

Janjic ZI. 2002. Nonsingular implementation of the Mellor-Yamada level 2.5 scheme in the NCEP Meso model. NCEP Office Note No. 437, 61 pp.

Kain JS, Fritsch JM. 1990. A one-dimensional entraining/detraining plume model and its application in convective parameterization. *J. Atmos. Sci.* **47**: 2784–2802.

Kain JS, Fritsch JM. 1993. Convective parameterization for mesoscale models: the Kain-Fritcsh scheme. In *The Representation of Cumulus Convection in Numerical Models*, Emanuel KA, Raymond DJ (eds). American Meteorological Society: Boston, MA. 246 pp.

Kessler E. 1969. *On the Distribution and Continuity of Water Substance in Atmospheric Circulation*, *Meteorological Monographs, Vol. 32*. American Meteorological Society: Boston, MA. 84.pp.

Lorenz E. 1963a. Deterministic nonperiodic flow. *J. Atmos. Sci.* **20**: 130–141.

Lorenz E. 1963b. The mechanics of vacillation. *J. Atmos. Sci.* **20**: 448–464.

Mellor GL, Yamada T. 1982. Development of a turbulence closure model for geophysical fluid problems. *Rev. Geophys. Space Phys.* **20**: 851–875.

Mendes D, Souza EP, Marengo JA, Mendes MCD. 2010. Climatology of extratropical cyclones over the South American–southern oceans sector. *Theor. Appl. Climatol.* **100**: 239–250, DOI: 10.1007/s00704-009-0161-6.

Patil DJ, Hunt BR, Kalnay E, Yorke JA, Ott E. 2001. Local low dimensionality of atmospheric dynamics. *Phys. Rev. Lett.* **86**: 5878–5881, DOI: 10.1103/PhysRevLett.86.5878.

Possia N, Cerne B, Campetella C. 2003. A diagnostic analysis of the Río de la Plata superstorm, May 2000. *Meteorol. Appl.* **10**: 87–99.

Sinclair MR. 1995. A climatology of cyclogenesis for the Southern Hemisphere. *Mon. Weather Rev.* **123**: 1601–1619.

Skamarock WC, Klemp JB, Dudhia J, Gill DO, Barker DM, Duda MG, Huang X, Wang W, Powers JG. 2008. A description of the advanced research WRF version 3. NCAR Technical note NCAR/TN-475+STR, 113 pp.

Skamarock WC, Klemp JB, Dudhia J, Gill DO, Barker DM, Wang W, Powers JG. 2005. A description of the advanced research WRF version 2. NCAR Tech. Note NCAR/TN-468&STR, 88 pp.

Tan Z, Zhang F, Rotuno R, Zinder C. 2004. Mesoscale predictability of moist baroclinic waves: experiments with parameterized convection. *J. Atmos. Sci.* **61**: 1794–1804.

Vera C, Vigliarolo PK, Berbery EH. 2002. Cold season synoptic scale waves over subtropical South America. *Mon. Weather Rev.* **130**: 684–699.

Wilks DS. 1995. *Statistical Methods in the Atmospheric Sciences – An Introduction*, *International Geophysics Series, Vol. 59*. Academic Press: San Diego, CA. 467 pp.

Zhang F, Snyder C, Rotuno R. 2002. Mesoscale predictability of the "surprise" snowstorm of 24–25 January 2000. *Mon. Weather Rev.* **130**: 1617–1632.

Zhu H, Thorpe A. 2006. Predictability of extratropical cyclones: the influence of initial condition and model uncertainties. *J. Atmos. Sci.* **63**: 1483–1497.

